OPTICAL MATERIALS 1 (1992) 177–184
North-Holland

Optically written waveguides in ion implanted $Bi_4Ge_3O_{12}$

W.S. Brocklesby, S.J. Field, D.C. Hanna, A.C. Large, J.R. Lincoln, D.P. Shepherd, A.C. Tropper
Department of Physics and Optoelectronics Research Centre, University of Southampton, Southampton SO9 5NH, UK

P.J. Chandler, P.D. Townsend, L. Zhang
School of Mathematical and Physical Sciences, University of Sussex, Brighton BN1 9QH, UK

X.Q. Feng and Q. Hu
Shanghai Institute of Ceramics, Chinese Academy of Sciences, Shanghai 200050, China

Received 9 March 1992

We report the first observation of optically written channel waveguides in ion implanted $Bi_4Ge_3O_{12}$ (BGO). Raman spectroscopy has been used to investigate the changes occurring due to both the original ion implantation and the subsequent optical writing of channel waveguides.

1. Introduction

The electro-optic crystal $Bi_4Ge_3O_{12}$ (BGO), [1], is known to form low loss waveguides when implanted with He^+ ions, [2–5], and can readily be doped with rare earth ions for laser applications, [6,7]. These attributes have provided motivation for the study of ion-implanted BGO waveguide lasers [7]. Here we report on the unexpected observation of optically written channel waveguides in ion-implanted BGO. This novel effect has been observed and repeated many times in both rare-earth doped and undoped BGO crystals. The ability to optically write channel waveguides may have a significant impact on the construction of complex waveguide circuits.

In order to determine the physical structure of the BGO waveguiding medium, both in the standard ion implanted planar guides and the optically written channel guides, extensive Raman scattering measurements are undertaken. The use of a high resolution Raman microprobe enables accurate comparisons of the structure of the bulk crystal and ion implanted regions. From these comparisons evidence of changes to the crystal structure upon ion implantation are discussed and related to the unusual refractive index properties of ion implanted BGO. Furthermore, it is possible to use the high intensity laser light available with the Raman microprobe to optically write channel waveguides into the ion implanted region. It is thus possible to study changes in the Raman spectra of these channels using the same experimental set-up to both write and probe the channels without the necessity to re-align the sample. The effects of channel writing on the Raman spectra of the BGO are thus reported on here where it is guaranteed that the modified guiding region is probed.

2. Ion-implantation effects in BGO crystals

Implantation of He^+ ions into dielectric crystals is known to cause refractive index changes suitable for the formation of planar optical waveguides, [8]. The He^+ ions travel through the crystal initially being slowed by electronic excitation. The depth of this 'electronic stopping region' depends on the initial energy of the ions. Nuclear collision events become significant at the end of the ion track, the 'nuclear

stopping region', when the ions have been slowed sufficiently to deposit the last ~ 100 keV of their energy. Nuclear collisions lead most commonly to an index reduction in the nuclear stopping region and this is sometimes accompanied by an increase of index in the electronic stopping region. Both of these effects can lead to optical confinement, with the guided wave being confined predominantly in the electronic stopping region. The crystal is generally annealed after implantation to reduce the propagation loss by removing absorption associated with colour centres formed during the implant.

The BGO crystals used in these experiments were implanted at 77 K with 4×10^{16} He^+ ions cm^{-2} at an energy of 1.5 MeV, and were subsequently annealed for 30 minutes at 200 °C. Such an implant produces the refractive index profile shown in fig. 1a of ref. [4], giving in this case an index increase of 0.9% in the electron stopping region which rises to 2.0% in the nuclear stopping region. These implant conditions were selected to be appropriate for 1.064 μm operation of a Nd:BGO waveguide laser, [7]. The rare-earth doping appeared to have no effect upon either the ion-implanted waveguide properties or the optically written channel waveguides to be described later.

A Raman scattering study was carried out on an undoped ion-implanted BGO crystal. Figure 1a shows the Raman spectrum of bulk crystalline BGO. The spectrum shown was obtained using a micro-Raman probe utilising a 514.5 nm argon laser line and exciting an area of around 2 μm^2 on the surface of the BGO crystal several millimetres away from the ion implanted region. The crystallographic orientation of the sample was unknown but was kept constant with respect to the incident laser direction and polarisation throughout the following measurements. The spectrum shown in fig. 1a agrees well with that given by Couzi et al., [9], who have also assigned mode vibrations to the various peaks.

To obtain the Raman spectrum from the waveguiding/ion implanted region of the BGO crystal the sample was moved so that the polished end of the waveguide was probed by the Raman system. This alignment was achieved by observing the magnified image of the end of the guide and manipulating the sample until the probing laser light was launched into the waveguide. The bulk Raman spectrum given in

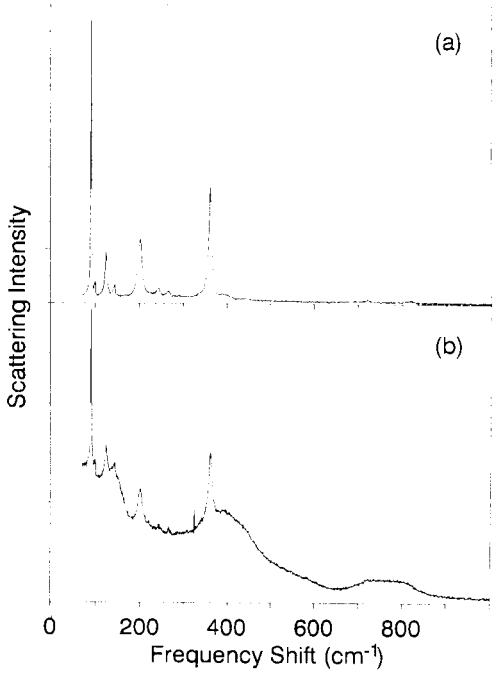

Fig. 1. (a) Raman spectrum of bulk BGO crystal excited with a 514.5 nm Ar^+ laser. (b) Raman spectrum taken under the same experimental conditions as (a), but probing the waveguiding region of the ion-implanted BGO crystal.

fig. 1a was obtained by a coarse adjustment moving the sample such that the laser probe was in the bulk crystal. Figure 1b shows the resultant Raman spectrum from the waveguiding region of the ion implanted BGO. From comparison of the spectra in fig. 1a and fig. 1b it can be seen that a large background with some broad peaks has arisen in the ion implanted region. As the probe light is being efficiently coupled into the guide, the Raman spectra collected will be from both the electronic and nuclear stopping regions.

To elucidate the nature of the background evident in fig. 1b the spectrum from the bulk BGO given in fig. 1a was scaled so that the heights of the crystal peaks matched the peak heights above background observed in the spectrum from the ion implanted region. The scaled bulk Raman spectrum was then subtracted from the Raman spectrum of the ion implanted region. The result is shown in fig. 2a and can be compared to fig. 2b, the Raman spectrum of bulk bismuth germanate glass with 60% GeO_2 40% $BiO_{1.5}$,

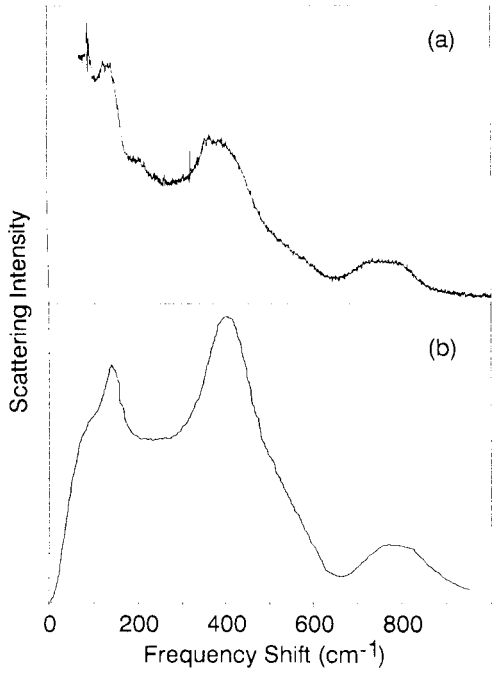

Fig. 2. (a) The result of subtracting the Raman spectra of the bulk BGO, fig. 1a, from the Raman spectra from the ion implanted region, fig. 1b, having linearly scaled the bulk spectrum so that the heights of the bulk crystalline peaks match the heights of the crystal peaks, above background, seen in the Raman spectra from the ion implanted region. (b) Raman spectrum of bulk BGO glass with 40% Bi 60% Ge, taken from Miller et al. [9].

taken from Miller et al. [10]. Above 100 cm^{-1} the two Raman spectra, from bulk bismuth germanate glass and the background from the ion implanted crystal, are remarkably similar and differ only very slightly in peak positions and widths, suggesting that ion implantation and subsequent annealing has substantially amorphized the BGO crystal. The tendency of the background Raman scattering, fig. 2a, to increase below 100 cm^{-1} rather than tend to zero, as seen in the spectra of Miller et al., fig. 2b, is because Miller et al. have reduced their Raman spectra to absolute zero [10] where as fig. 2a is uncorrected at 300 K.

Amorphization on ion implantation, which has been frequently demonstrated in ion implanted semiconductors [11] and insulators [8], is not surprising in itself and has been postulated as the mechanism for waveguide formation in a number of ion implanted dielectric crystals showing refractive index lowering at the end of the ion track, [8]. The composition of the original BGO crystal ($Bi_4Ge_3O_{12}$) equivalent to 57% $BiO_{1.5}$ 43% GeO_2 is also known to be within the stoichiometries capable of bulk glass formation [12], although at the high concentration extreme of $BiO_{1.5}$. BGO is somewhat exceptional since it shows a refractive index enhancement at the end of the ion track, rather than the lowering normally associated with the rarefaction of a matrix on amorphization. However, as indicated by Townsend, [8], changes in the optical absorption or bond polarisabilities of a material on amorphization can cause an increase in the refractive index. Indeed, the refractive index of bismuth/thallium lead/antimony germanate glasses has been observed by Wood et al. [13] to increase with movements of the ultra-violet (uv) absorption edge to longer wavelengths. In binary bismuth germanate glass the uv absorption edge is mainly defined by absorption in the bismuth from the $^1S_0$ electronic level to $^3P_0$ or $^3P_1$ levels [14]. Boulon et al. have further demonstrated that the position of the ^3P levels can vary by up to 4200 cm^{-1} according to the local environment of the bismuth. We expect that when crystalline BGO is amorphized on ion implanted the local environment of the bismuth will change drastically, thus changing the uv absorption edge and therefore enhancing the refractive index.

To further study the effects of ion implantation on the BGO crystal, and any effects on the crystalline Raman features still evident in fig. 1b, further high resolution Raman spectra were taken from the bulk and guiding regions of the same ion implanted sample. To ensure that any peak shifts could be detected the high resolution Raman spectra were taken using the spectral coverage of a single CCD image thus avoiding any mechanical movement of the triple grating spectrometer and ensuring the absence of any backlash errors which are possible with a more standard single channel scanning spectrometer. The total spectral range of the high resolution spectra was therefore limited by the spectral coverage of the CCD detector, some 310 cm^{-1} at the wavelengths used here.

The resultant high resolution Raman spectra from the bulk BGO crystal and the waveguiding region are shown in figs. 3a and 3b, respectively. The incident and collection optics and position of the triple grat-

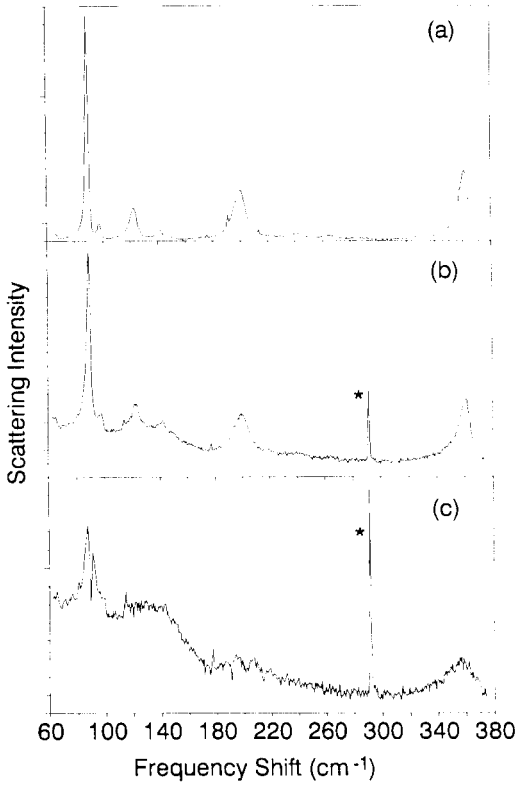

Fig. 3. High resolution Raman spectra of BGO in the bulk, (a), and ion-implanted, (b), regions, excited with a 514.5 nm Ar^+ laser. (c) is a subtraction of the bulk spectrum from the ion implanted spectrum, having scaled the bulk spectrum so that the heights of the crystal peaks match the crystal like peak heights, above background, from the ion implanted region. Features marked '*' are cosmic ray noise.

ing spectrometer remained unchanged between the two spectra with the sample position the only variable changed. Scaling the bulk Raman spectrum peak heights to match those from the waveguide and subtracting from the waveguide spectrum yields fig. 3c. The subtraction reveals the amorphous background noted above, together with an incomplete cancellation of the crystalline peak wings, most clearly seen in the 75 cm^{-1} peak. This indicates a significant broadening of the crystalline Raman scattering component within the waveguide. The asymmetry of the difference spectrum around the original line centre could be due to either asymmetric broadening of the Raman line or a small frequency shift of the peak Raman intensity. The dominant mechanism cannot be determined from this spectrum, although if a peak shift is present it must certainly be less than ~ 1 cm^{-1} as any greater shift would be detectable from comparing the guide and bulk spectra.

The causes of the peak broadening shown in fig. 3c are unclear. The formation of microcrystals is a possible explanation of the peak broadening although in ion-implanted GaAs this however, is associated with both peak broadening and peak shifts, [11], the peak shifts are dependent on the presence of a rapidly varying phonon dispersion curve for the material, [15], and thus microcrystals could be responsible for the observed peak broadening in BGO if the phonon dispersion curve in this material is flat.

3. Optical writing of channel waveguides

The observation of channel waveguide formation by end-launching of a laser beam into a planar ion-implanted BGO waveguide was an unexpected effect. An argon-ion laser operating on all lines was end launched into a Nd^{3+} doped BGO planar waveguide and the output from the guide was focused onto a beam profile analyzer, (Big Sky Software Corporation beamview analyser). At low pumps powers ($\leqslant 30$ mW) the output appears as in fig. 4a, showing the expected wide gaussian shape resulting from the beam expansion in the unguided (horizontal) plane. The spot size ($1/e^2$ half-width of intensity) at the output end of the waveguide is ~ 120 μm. Figures 4b–f show how the output profile varies with increasing power. Between 30 and 75 mW there is a very dramatic narrowing of the profile in the horizontal plane. Beyond this point the profile shows a much slower narrowing up to powers of 350 mW. Thus some self-focusing effect appears to have taken place effectively forming a channel waveguide with an output spot size of ~ 10 μm. The spot size in the vertical plane is unchanged. The index change causing this self-focusing appears to be permanent as shown in fig. 5. Here we compare the output profiles with the same pump power (too low to form channels itself), before and after channel fabrication. It is also possible to move the launch position horizontally along the waveguide and observe the output profile change between planar and channel propagation. An end launched HeNe beam also showed

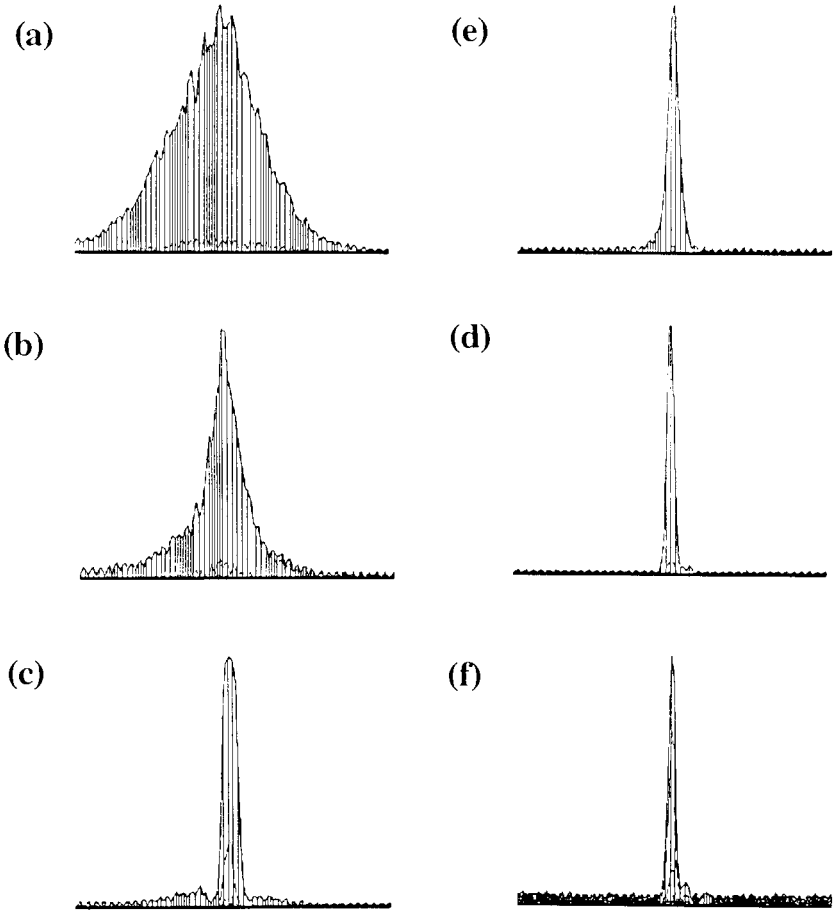

Fig. 4. Waveguide output profiles with increasing pump power; (a) 30 mW, (b) 55 mW, (c) 75 mW, (d) 95 mW, (e) 130 mW, (f) 350 mW.

channel propagation in the guides previously written by the argon beam. Figure 5b shows that launching into the channel with powers lower than that necessary to create these guides gives output profiles with low level side wings. This may be due to the fact that we are launching with a circular spot when the mode of the channel guide is actually much larger in the horizontal plane than the vertical plane. We observed similar effects in undoped ion-implanted BGO waveguides but no effect occurred in the bulk crystal (doped or undoped) up to pump powers of 3 W.

The observed effects were not consistent with photorefractive damage (which can occur for certain phases of the Bi_2O_3–GeO_2 system). To confirm this the channel waveguide was illuminated with a strong white light source for 1 hour. There was no observed effect upon the output profile (pumping at low power) indicating that photorefractive damage is not the cause of the channel formation. As the argon-ion pump light is strongly absorbed by the BGO crystal it is possible that the thermal load is causing the index change. This is consistent with the observation that there was a much higher threshold for channel formation when pumping with an R6G dye laser tuned just off the strong 590 nm Nd absorption ($\sim$200 mW) than on it ($\sim$50 mW).

By pumping at wavelengths tuned off the Nd absorption we were able to measure the transmission (including both the propagation loss and launch efficiency) of the 5 mm long channels. At low powers

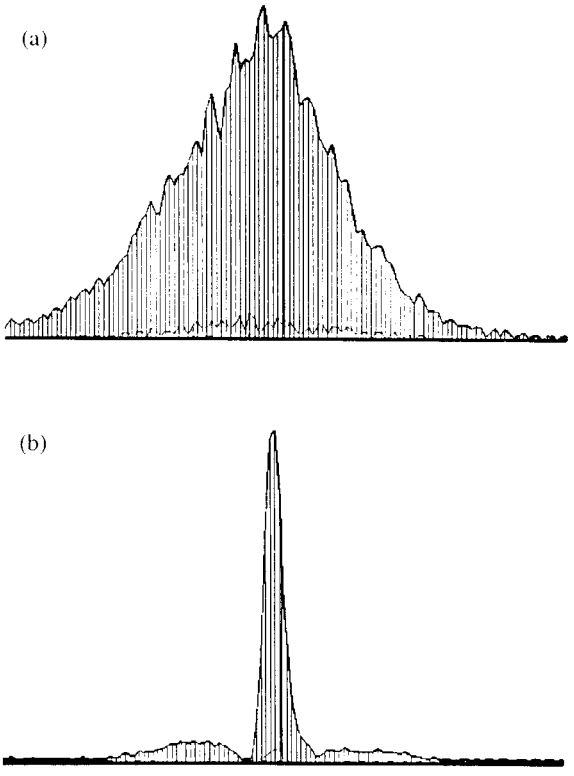

Fig. 5. Waveguide output profiles before and after channel waveguide fabrication for a pump power of 30 mW.

the ordinary planar waveguide transmission was 60%. At powers high enough to form channels the transmission was 50% and virtually all the power was in the narrowed profile. Launching low powers into the already formed channel guide still gave overall transmissions of 50% but now only half the power was contained within the narrowed profile, the rest being contained in the side wings.

Some initial trials were also carried out on writing channels with a beam focused on the top surface of the guide. The potential usefulness of the guides would obviously be much enhanced if such a procedure were possible, allowing the writing of complicated circuits including curved guides. By tracking the planar waveguide through the path of an argon-ion beam we were able to write 'lines' which were visible to the eye under a microscope. However as yet we have been unable to end-launch light into these 'lines'. An investigation to establish the appropriate pump power and spot size needed to create guides capable of supporting waveguide modes at the required wavelengths is currently in progress.

We have conducted a Raman investigation of the nature of the (end-launched) optically written waveguides. Again high resolution Raman spectra were taken in the waveguide region, utilising the coverage of a single CCD image. The first spectrum was taken using the 488 nm Ar^+ laser line at low power, ($\sim$30 mW), the result is shown in fig. 6a and is equivalent to fig. 3b which was taken with the 514.5 nm Ar^+ line. Due to lack of availability of an interference filter at 488 nm, plasma lines emitted

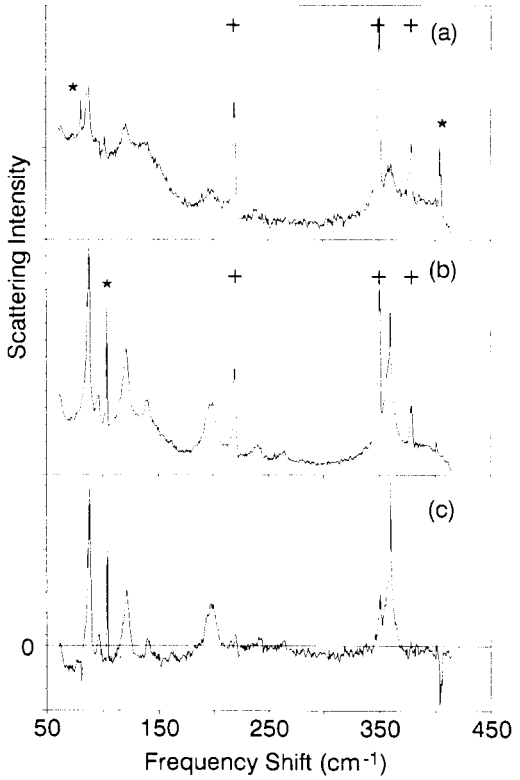

Fig. 6. Raman spectra of the ion-implanted region before, (a), and after, (b), optically writing a channel waveguide, excited with 30 mW of a 488 nm Ar^+ laser. Both (a) and (b) are plotted on the same horizontal and vertical scales. (c) Direct subtraction of the Raman spectra before optically writing a guide (a) from the spectra after optically guide writing (b), showin an increase in the crystalline component of the Raman spectrum after optically writing the channel guide. Features marked '*' are cosmic ray noise. Those marked '+' and appearing in (a) and (b) are plasma lines from the Ar^+ laser. The subtraction means the latter do not appear in (c).

from the argon laser appear, along with the Raman spectra, in figs. 6a and 6b and are marked with a '+' sign. Immediately following the recording of the Raman spectra of fig. 6a the laser power was increased to ~120 mW without moving the sample and thus still probing the ion-implanted region. Following the exposure to the higher power laser, the light emerging from the waveguide was observed to have become spatially more confined, indicating the optical writing of a channel waveguide as described earlier. Following the writing of a waveguide the power of the incident 488 nm laser light was reduced to the same level as that before writing, (~30 mW), and another Raman spectrum recorded. The result is shown in fig. 6b. Throughout this sequence the position of the sample and spectrometer remained unchanged, thus ensuring the same area of the sample was probed before, during and after guide writing.

The Raman spectrum after guide writing, shown in fig. 6b, is on the same scale as fig. 6a and from comparison of these two spectra it can be seen that the magnitude of the sharp crystal peaks has increased, whilst the amorphous background remains constant. A subtraction of fig. 6a from fig. 6b without scaling of either spectrum is shown in fig. 6c. Fig. 6c clearly illustrates the increase in the crystalline component of the Raman spectrum after optically writing a channel waveguide in the ion implanted region of the BGO crystal. It is important to note that the increase in the crystalline component of the spectra is not merely due to a spreading of the mode further into the crystal substrate when propagating in the optically written channel, as no such change in the vertical mode size was observed experimentally.

The increase of the crystalline component in the Raman spectral would appear to indicate a change of structure toward that of the original crystal prior to ion implantation. However, if this were the case one would assume the refractive index would return toward that of the bulk crystal, i.e. decrease, but such a refractive index decrease would not confine the light to a channel waveguide. In order for the observed confinement to occur the refractive index must be increased on high power laser illumination. The material must therefore either tend toward an even greater extreme of that caused by ion implantation or form a new state. Both of these later suppositions seem to be in contradiction to the observed Raman results.

4. Summary

We have demonstrated a method for creating optically written channel waveguides in ion-implanted BGO. Initial experiments have also been carried out on 'top-writing' waveguides, which could lead to a relatively simple method for writing complicated waveguide circuits and curved waveguides. This may well have applications in integrated optics especially as BGO is a (weak) electro-optic crystal. Channel waveguide fabrication may also lead to enhanced performance of rare-earth doped ion-implanted BGO waveguide lasers and amplifiers. Detailed Raman spectroscopy measurements indicated some amorphization of the crystal due to the ion-implantation and conversely an enhanced crystal signal in the optically written channels. However an explanation for the necessary refractive index changes is not yet available.

Acknowledgements

This work has been supported by the Science and Engineering Research Council and J.R.L., S.J.F. and A.C.L. acknowledge SERC for provision of research studentships. We also gratefully acknowledge R.W. Eason for useful discussions.

References

[1] R. Nitsche, J. Appl. Phys. 36 (1965) 2358.
[2] S.M. Mahdavi, P.J. Chandler and P.D. Townsend, J. Phys. D: Appl. Phys. 22 (1989) 1354.
[3] S.M. Mahdavi and P.D. Townsend, J. Chem. Soc. Faraday Trans. 86 (1990) 1287.
[4] S.M. Mahdavi and P.D. Townsend, Electron. Lett. 26 (1990) 371.
[5] S.M. Mahdavi, G. Lifante and P.D. Townsend, to be published Nucl. Instrum. Methods B (1991).
[6] L.F. Johnson and A.A. Ballman, J. Appl. Phys. 40 (1969) 297.

[7] S.J. Field, D.C. Hanna, A.C. Large, D.P. Shepherd, A.C. Tropper, P.J. Chandler, P.D. Townsend and L. Zhang, in: OSA Proceedings on Advanced Solid State Lasers, vol. 10 (Optical Society of America, 1991) pp. 353–357.
[8] P.D. Townsend, Rep. Prog. Phys. 50 (1987) 501.
[9] M. Couzi, J.R. Vignalou and G. Boulon, Solid State Comm. 20 (1976) 461.
[10] A.E. Miller, K. Nassau, K.B. Lyons and M.E. Lines, J. Non-Cryst. Solids 99 (1988) 289.
[11] M. Holtz, R. Zallen, O. Brafman and S. Matteson, Phys. Rev. B 37 (1988) 4609.
[12] K. Nassau and D.L. Chadwick, J. Am. Ceram. Soc. 65 (1982) 197.
[13] D.L. Wood, K. Nassau and D.L. Chadwick, Appl. Optics 21 (1982) 4276.
[14] G. Boulon, B. Monie and J.-C. Bourcet, Phys. Rev. B 22 (1980) 1163.
[15] K.K. Tiong, P.M. Amirtharaj, F.H. Pollak and D.E. Aspnes, Appl. Phys. Lett. 44 (1983) 122.